

## RESEARCH ARTICLE

# Alternating Connectivity with Temporal Delays between the Pacific, Atlantic, and Indian Oceans

Fenyng Cai<sup>1,2</sup>, Song Yang<sup>3,4</sup>, Shuheng Lin<sup>5\*</sup>, and Tuantuan Zhang<sup>3,4</sup>

<sup>1</sup>Potsdam Institute for Climate Impact Research (PIK), Member of the Leibniz Association, P.O. Box 60 12 03, D-14412 Potsdam, Germany. <sup>2</sup>Department of Geography, Humboldt-Universität zu Berlin, 10099 Berlin, Germany. <sup>3</sup>School of Atmospheric Sciences, Sun Yat-sen University and Southern Marine Science and Engineering Guangdong Laboratory (Zhuhai), 519082 Zhuhai, China. <sup>4</sup>Guangdong Province Key Laboratory for Climate Change and Natural Disaster Studies, Sun Yat-sen University, 519082 Zhuhai, China. <sup>5</sup>Key Laboratory of Humid Subtropical Eco-geographical Process (Ministry of Education), College of Geographical Sciences, Fujian Normal University, 350108 Fuzhou, China.

\*Address correspondence to: [s.lin@fjnu.edu.cn](mailto:s.lin@fjnu.edu.cn)

Sea surface temperature (SST) variability interacts dynamically across the Pacific, Atlantic, and Indian oceans, exerting pronounced influence on global climate. However, the mechanism of signal transmission among these basins remains unclear. Using complex network analysis of lead–lag SST connections, results indicate that dominant interannual influences shift sequentially across the Pacific, Atlantic, and Indian oceans. At short-term lags ( $\leq 6$  months), the Pacific strongly affects the Indian Ocean. For medium-term lags (7 to 19 months), the Atlantic exerts greater influence on the Pacific. At long-term lags ( $\geq 20$  months), pronounced SST connections emerge from both the Indian and Pacific oceans toward the Atlantic. Coupled Model Intercomparison Project Phase 6 models capture short-term Pacific impacts effectively, but only a limited subset reproduces medium- and long-term interbasin linkages. Furthermore, model projections consistently suggest intensification of these cross-basin interactions under future warming scenarios. Quantitative evaluation of lead–lag signal flow among oceans enhances understanding of interbasin interactions and large-scale climate variability.

## Introduction

Oceans constitute a fundamental component of Earth's climate system, functioning as critical lower boundary conditions for the atmosphere. Owing to substantial heat capacity and strong thermal inertia, they regulate the atmospheric variability while serving as long-term reservoirs for climate signals across diverse time scales [1–3]. The Pacific, Atlantic, and Indian oceans together account for  $>70\%$  of the global ocean surface area. Given their dominant spatial coverage and dynamic influence, these basins have drawn substantial attention for their role in shaping regional and global climate variability [4–6].

The El Niño–Southern Oscillation (ENSO), originating in the tropical Pacific, remains the most prominent mode of interannual climate variability [7–10]. However, increasing evidence indicates that the variability in the Indian and Atlantic oceans can influence ENSO evolution and exert independent impacts on the global climate system [11–16]. This recognition has shifted research focus from single-basin analyses toward integrated interbasin or pantropical perspectives on climate variability and its mechanisms. Recent reviews have synthesized advances in understanding of interbasin interactions [4,5]. Sea surface temperature (SST) anomalies originating in one basin can affect remote basins via atmospheric bridges, including modifications to Walker and Hadley circulations and excitation

of planetary-scale stationary waves [17,18], as well as oceanic pathways such as the Indonesian Throughflow (ITF) [19]. For example, El-Niño-induced changes in the Walker circulation often produce a dipole-like SST pattern in the Indian Ocean, called the Indian Ocean dipole (IOD) during summer and autumn [20–22] and an Indian Ocean basin-warming mode (IOBM) during winter and spring [23–25]. The IOBM persists into the subsequent summer through El-Niño-induced oceanic Rossby waves and local air–sea interactions in the Indian Ocean [25]. Moreover, La Niña can trigger SST warming off the west coast of Australia by enhancing ITF, a phenomenon known as the Ningaloo Niño [26]. In turn, these Indian Ocean modes may accelerate El Niño decay or trigger a La Niña in subsequent years by strengthening equatorial Pacific winds [27–31] or increasing ITF transport, which modulates the heat content in the equatorial Pacific [32,33]. In addition, IOD-related rainfall anomalies near the Maritime Continent can generate atmospheric Rossby wave trains extending into the South Pacific mid-latitudes and further influence the extratropical Pacific climate [34,35].

Pacific and Atlantic interactions occur through similar mechanisms to those linking other basins. During El Niño decay in spring, tropical North Atlantic warming arises from the anomalous Walker circulation and local Hadley circulations [36,37] or from the subtropical cyclone that reduces trade winds via the Pacific North American pattern [38–41]. Tropical North

**Citation:** Cai F, Yang S, Lin S, Zhang T. Alternating Connectivity with Temporal Delays between the Pacific, Atlantic, and Indian Oceans. *Ocean-Land-Atmos. Res.* 2026;5:Article 0142. <https://doi.org/10.34133/olar.0142>

Submitted 24 September 2025  
Revised 3 March 2026  
Accepted 3 March 2026  
Published 2 April 2026

Copyright © 2026 Fenyng Cai et al. Exclusive licensee Southern Marine Science and Engineering Guangdong Laboratory (Zhuhai). No claim to original U.S. Government Works. Distributed under a Creative Commons Attribution License (CC BY 4.0).

Atlantic SST anomalies may initiate a La Niña event by strengthening Pacific trade winds through Rossby wave responses [13,42,43]. Moreover, equatorial Atlantic Niño has been suggested to influence ENSO evolution in subsequent seasons [44–48]. Significant interactions between the Indian and Atlantic oceans have also been documented. Tropical Atlantic warming induces easterly anomalies over the tropical Indian Ocean through Kelvin wave responses, promoting warming by reducing coastal upwelling and surface evaporation [49–51]. Conversely, a positive IOD may trigger westerly anomalies over the equatorial Atlantic via westward-propagating Rossby waves, favoring Atlantic Niño development in the subsequent summer [52]. Beyond tropical processes, subtropical and mid-latitude SST variability also contributes to interbasin climate interactions. For example, atmospheric and SST anomalies over the North Pacific during boreal winter and spring, such as the North Pacific Oscillation and Pacific Meridional Mode, have been shown to influence ENSO evolution by modulating equatorial trade winds [53,54]. Similarly, subtropical North Atlantic SST variability, including the Atlantic tripole mode, can affect ENSO by altering mid-latitude atmospheric and oceanic circulation through downstream-propagating Rossby wave trains [55].

Despite notable progress, significant gaps persist in understanding the timing and directionality of interactions among the 3 oceans. Most previous studies [12,13,23,42] have used composite analyses or lagged cross-correlation and regression techniques to explore interbasin relationships. These conventional approaches, often reliant on predefined climate indices, are highly sensitive to regional selection and may overlook the complexity of interactions among diverse climate modes [56–58]. Particularly for long-delayed signals, significant links exist among different grid cells, but these significant signals are often neglected in conventional statistical analyses. Sensitivity experiments using climate models are also widely applied to investigate interbasin dynamics; however, their reliability is constrained by persistent model biases, particularly in simulating ENSO characteristics and the mean state of tropical SST [6,59–62]. High computational costs and uncertainties in the parameterizations further limit feasibility and robustness. These challenges emphasize the need for data-driven approaches capable of comprehensively detecting and quantifying lead-lag linkages across remote ocean basins.

To address these challenges, a complex network methodology was applied to investigate the lead-lag connectivity among the Pacific, Indian, and Atlantic oceans on interannual time scales. Complex network analysis provides a robust data-driven framework for uncovering intricate linkages within a climate system without relying on predefined indices. Previous studies have demonstrated its utility in revealing remote teleconnection pathways, such as propagating atmospheric signals linking remote occurrences of extreme rainfall [63,64] and heat waves [65,66], as well as identifying key tropical convection regions driving global atmospheric variability [67]. In addition, complex networks have been utilized to characterize the topology of SST anomalies in the Pacific [68,69] and Indian [70] oceans. However, its application to diagnose interactions among the Pacific, Indian, and Atlantic oceans remains limited. In this study, time-lagged networks of observed SSTs were constructed to systematically trace influence flows across the 3 basins. This approach allowed identification of leading and lagging regions, quantification of propagation delays, and mapping interbasin signal pathways, thereby providing a dynamically informed perspective on multibasin coupling and its broader climate implications.

## Materials and Methods

### Datasets

Monthly SST data for 1979–2023 were derived from the HadISST1 dataset [71]. Furthermore, monthly SST outputs from 34 climate models participating in the Coupled Model Intercomparison Project Phase 6 (CMIP6) [72] were analyzed, including historical simulations for 1979–2014 and future projections under the SSP5-8.5 scenario for 2064–2099. Only the first realization (r1i1p1f1, or r1i1p1f2/r1i1p1f3 when r1i1p1f1 is unavailable) of each model was adopted. Brief information about the 34 CMIP6 models is provided in Table S1. To extract SST anomalies for network analysis, both observational and model-simulated SST data were interpolated onto a  $2^\circ \times 2^\circ$  horizontal grid, removing seasonal cycle and long-term trends.

### Network analysis and signal flow among the 3 oceans

In this study, 37 networks were constructed for time lags ranging from 0 to 36 months. For each pair of grid cells,  $a$  and  $b$ , the link strength  $A_{i,(a,b)}$  was defined as the correlation coefficient between monthly SST anomalies at the 2 locations, with grid cell  $a$  leading grid cell  $b$  by  $i$  months. Only statistically significant correlation coefficients ( $P < 0.05$ ) were retained in the network. The analysis domain was confined to  $60^\circ\text{S}$  to  $60^\circ\text{N}$  to exclude regions that may have been covered by polar ice.

Signal transmission among the Pacific, Atlantic, and Indian oceans was quantified using total degree centrality. At time lag  $i$ , the total degree centrality from region  $A$  to  $B$  was defined as the sum of significant links across all grid cells in the 2 regions:

$$D_{i,(A \rightarrow B)} = \sum_{a \in A, b \in B} (A_{i,(a,b)} * W_{(a,b)}) \quad (1)$$

Here,  $D_{i,(A \rightarrow B)}$  is the total degree centrality, and  $W_{(a,b)} = \cos\left(\frac{(|\text{lat}_a| + |\text{lat}_b|)}{2}\right)$  is a weight coefficient for a link between grid points  $a$  and  $b$ . For example,  $D_{i,(\text{Pacific} \rightarrow \text{Atlantic})}$  indicates the strengths of signal transport from the Pacific to the Atlantic when the Pacific signal preceded the Atlantic signal by  $i$  months. The degree of divergence of ocean region is defined as the net signal flow, calculated as the difference between signals originating from and signals received by that region. For example, the degree of divergence of the Pacific was identified as

$$\Delta D_{i,(\text{Pacific})} = D_{i,(\text{Pacific} \rightarrow \text{Atlantic})} + D_{i,(\text{Pacific} \rightarrow \text{Indian})} - D_{i,(\text{Atlantic} \rightarrow \text{Pacific})} - D_{i,(\text{Indian} \rightarrow \text{Pacific})} \quad (2)$$

Positive  $\Delta D_i$  indicates that the region acts as a source of interbasin signals, whereas a negative value indicates a sink. At zero lag ( $i = 0$ ), the degree of divergence is zero because no temporal precedence is defined.

### Singular value decomposition analysis

To assess the robustness of complex network analysis outcomes, singular value decomposition (SVD) was applied to SST anomaly fields across paired ocean basins at specific time lags. Specifically, three SVD analyses are conducted: (a) between Pacific SST anomalies (1979 January to 2020 December) and Indian Ocean SST anomalies with a lag of 3 months (1979 April to 2021 March);

(b) between Atlantic SST anomalies (1979 January to 2020 December) and Pacific SST anomalies with a lag of 12 months (1980 January to 2021 December); (c) between Indian Ocean SST anomalies (1979 January to 2020 December) and Atlantic SST anomalies with a lag of 24 months (1981 January to 2022 December).

**Results**

**Alternating signal flow among the Pacific, Atlantic, and Indian oceans**

Global oceans between 60°S and 60°N are geographically separated into 3 major basins: Pacific, Atlantic, and Indian (Fig. 1B to D) oceans. The Arctic Ocean was excluded because of persistent sea ice cover. Signal flow among these basins was quantified by evaluating total degree centrality across varying time lags. Specifically, the degree of divergence is calculated as the difference between the signals of one ocean that precede and lag those of the other ocean basins. Positive divergence denotes a basin acting as a source of signals, while negative divergence indicates a sink within interbasin interactions. Alternating dominant influences were identified across the Pacific, Atlantic, and Indian oceans (Fig. 1A). During the initial 6 months (short-lag period), signal transmission was primarily directed from the Pacific Ocean to the Indian Ocean (Figs. 1A and 2A and D). This result is likely manifested as a short-lag influence of ENSO in the tropical Pacific on the IOBM. The IOBM often emerges during the boreal spring and summer, following the mature phase of ENSO in the preceding winter.

With delays exceeding 1 year, Pacific influence weakened, while Atlantic-to-Pacific signal flows emerged as the dominant mode during lags of 7 to 19 months (medium-lag period) (Figs. 1A and 2B and E). This feature likely reflects the role of tropical North Atlantic warming in the boreal spring in initiating La Niña events later in the year. Warming of the equatorial Atlantic may also contribute, as Atlantic Niño events peaking in summer can trigger La Niña development in the subsequent year. It has been suggested that Atlantic Niño events peaking in summer have the potential to trigger La Niña events in the following winter [44], whereas those peaking in the boreal winter may lead to La Niña development in the subsequent year [45]. Furthermore, La Niña events tend to persist and intensify in the second year [73,74], potentially contributing to the extended lead of the Atlantic Ocean signals over the Pacific, with influences lasting beyond 12 months. Moreover, the influence of the Atlantic Ocean on the Indian Ocean exhibited a medium-term lag (Fig. 2C). This is consistent with a previous study [4], which indicates that the Atlantic influences on the Indo-Pacific have strengthened, leading to an intensification of tropical Pacific cooling and Indian Ocean warming.

At longer lags of 20 to 36 months, significant flows were detected from the Indian and Pacific oceans toward the Atlantic Ocean (Figs. 1A and 2C and F). These long-delayed signals remain rarely addressed in previous studies and are discussed further in the following section.

**Possible physical mechanisms**

The spatial configuration of sequential ocean impacts is illustrated across the 3 basins. During the short-lagged intervals,

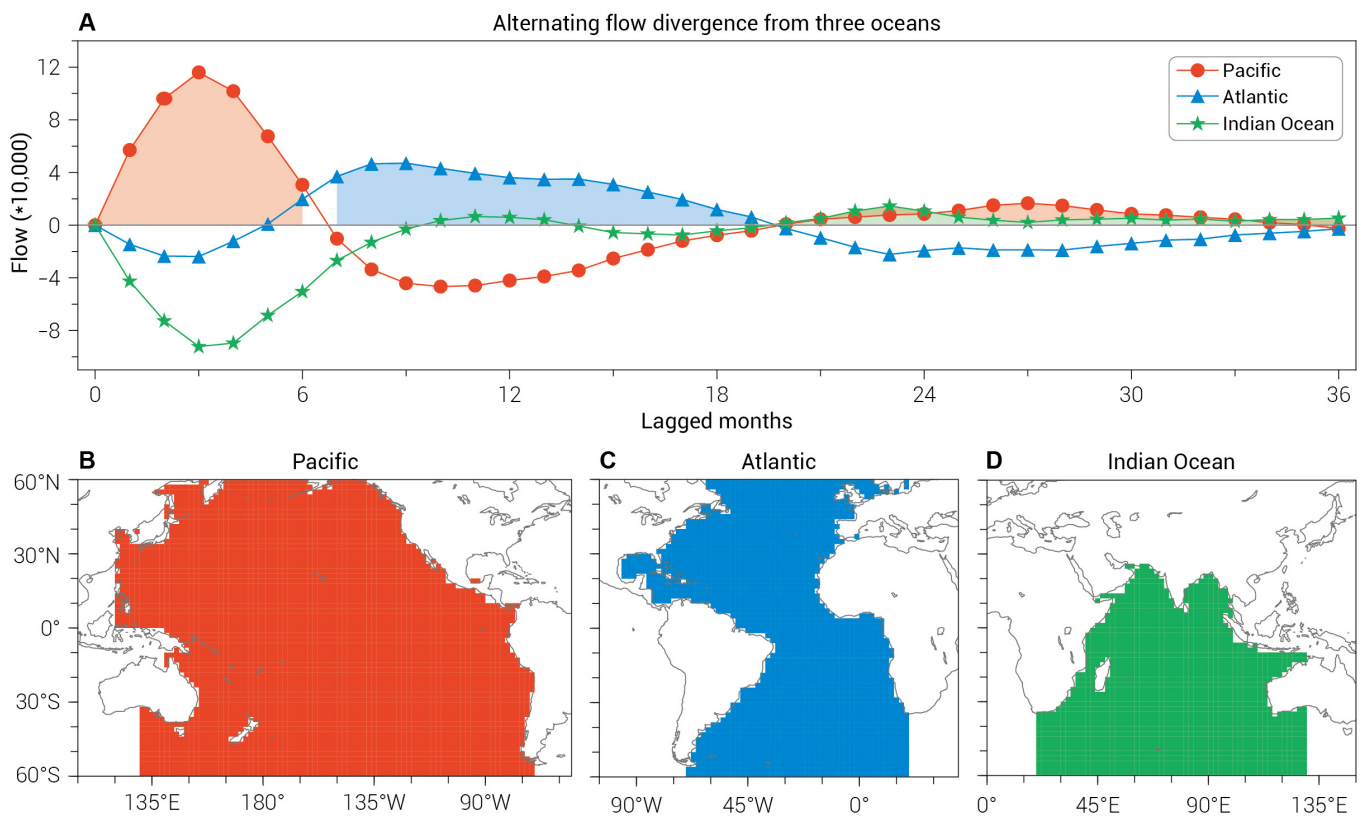


**Fig. 1.** Alternating dominances of signal transport from the Pacific, Atlantic, and Indian oceans in sequences. (A) Network degree divergence of the Pacific Ocean (red line with circles), the Atlantic Ocean (blue line with triangles), and the Indian Ocean (green line with pentagrams). Red, blue, and green grid cells ( $2^\circ \times 2^\circ$ ) belong to (B) the Pacific, (C) the Atlantic, and (D) the Indian Ocean, respectively.

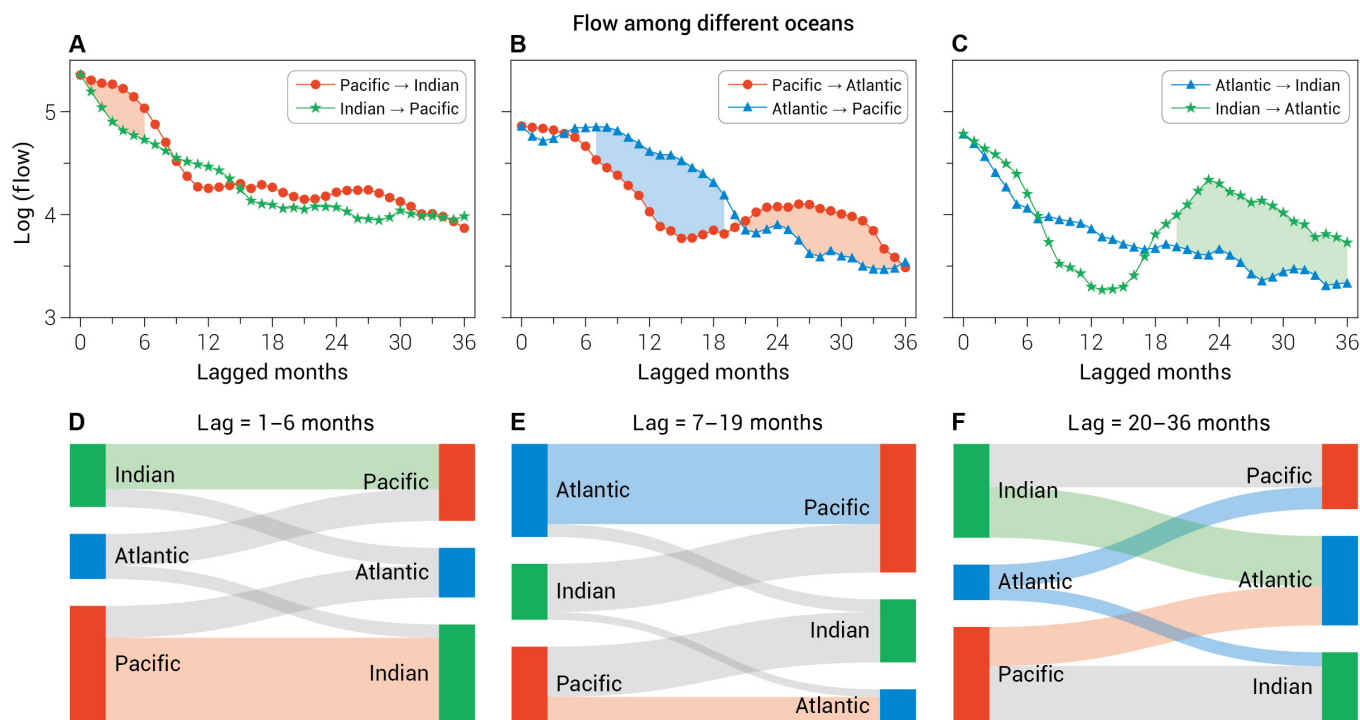


**Fig. 2.** Signal flow for 3 time-lag periods. Degree flow from (A) the Pacific Ocean to the Indian Ocean (red line with circles) and the Indian Ocean to the Pacific Ocean (green line with pentagrams). (B) the Pacific Ocean to the Atlantic Ocean (red line with circles) and the Atlantic Ocean to the Pacific Ocean (blue line with triangles), and (C) the Atlantic Ocean to the Indian Ocean (blue line with triangles) and the Indian Ocean to the Atlantic Ocean (green line with pentagrams). Degree flow among 3 oceans at lags of (D) 1 to 6 months, (E) 7 to 19 months, and (F) 20 to 36 months.

warm SST anomalies in the tropical central–eastern Pacific trigger basin-wide SST warming in the tropical Indian Ocean, with a lag of 3 months (Fig. 3A and B). This mechanism has been widely discussed in previous studies; El Niño events tend to induce IOBM during spring and summer following a mature winter through the modulation of the Walker circulation [23–25]. In particular, the Niño 3.4 index exhibits significant correlations with Indian Ocean SST anomalies at lags of 1 to 6 months, indicating a robust lead–lag relationship (Fig. 3C). This is consistent with our complex network analyses, which revealed numerous significant links between the SST grid cells in the Pacific and Indian oceans at lags of 0 to 6 months (Fig. 4A), further supporting the robustness of the complex network approach.

A 12-month-lagged linkage between tropical Atlantic warming encompassing the tropical North Atlantic and the equatorial Atlantic and tropical central–eastern Pacific cooling was identified through the SVD analysis (Fig. 3D and E). Springtime warming in the tropical North Atlantic tends to trigger La Niña events in the subsequent winter via an atmospheric Rossby wave response over the subtropical northeastern Pacific [13]. Atlantic Niño events peaking in summer or winter may also trigger La Niña by modulating the Pacific–Atlantic branch of the Walker circulation [45,75]. These lead–lag relationships may also be dynamically mediated by the propagation of large-scale sea level pressure and wind anomalies induced by Atlantic SST forcing, which propagates eastward across the Indian Ocean into the Pacific and modulate the Walker circulation [76]. Beyond tropical connections, significant correlations were observed between tropical Atlantic SST anomalies and those in the subtropical northeastern and southern Pacific, with a lag of nearly 1 year (Fig. 3F). Network analysis further showed that

certain links between the gridded SST anomalies in the tropical Atlantic and those in the subtropical northeastern Pacific and subtropical southern Pacific could persist for up to 13 to 18 months after tropical Atlantic warming (Fig. 4B). The northeastern Pacific signal may reflect prolonged La Niña conditions exceeding more than 1 year, whereas the mechanism underlying the tropical Atlantic and subtropical southern Pacific connection remains unclear and lies beyond the scope of this study.

A remote linkage between the tropical Indian Ocean and the subtropical southwestern Atlantic was identified with lags of approximately 2 years (Fig. 3G to I). These long-delayed connections appear mediated by the tropical northwestern Pacific and subtropical southwestern Pacific (Fig. 4C). This long-delayed signal emerged from a relay of 2 sequential 1-year-lagged links, effectively integrating and transmitting the signal over time (Fig. 4C).

The 1-year lag between the Indian Ocean and the tropical northwestern Pacific may be reflecting the tropospheric biennial oscillation (TBO). Previous studies suggest that SST linkage between these 2 regions on biennial time scales could be driven by interactions between the Asian monsoon system and Indo–Pacific air–sea coupling, which form the basis of the TBO mechanism [77–79]. The connection between the tropical northwestern Pacific and the subtropical southwestern Atlantic may involve the development of ENSO, with SST-related convection over the former region acting as a trigger of ENSO [80–82]. Once the ENSO matures, it can induce Rossby wave trains that propagate toward the subtropical South Atlantic [17], thereby establishing a delayed teleconnection. As for the Indian–subtropical southwestern Pacific pathway, a 2-stage oceanic process may offer a possible explanation. The SST anomalies in the Indian Ocean may influence the subtropical

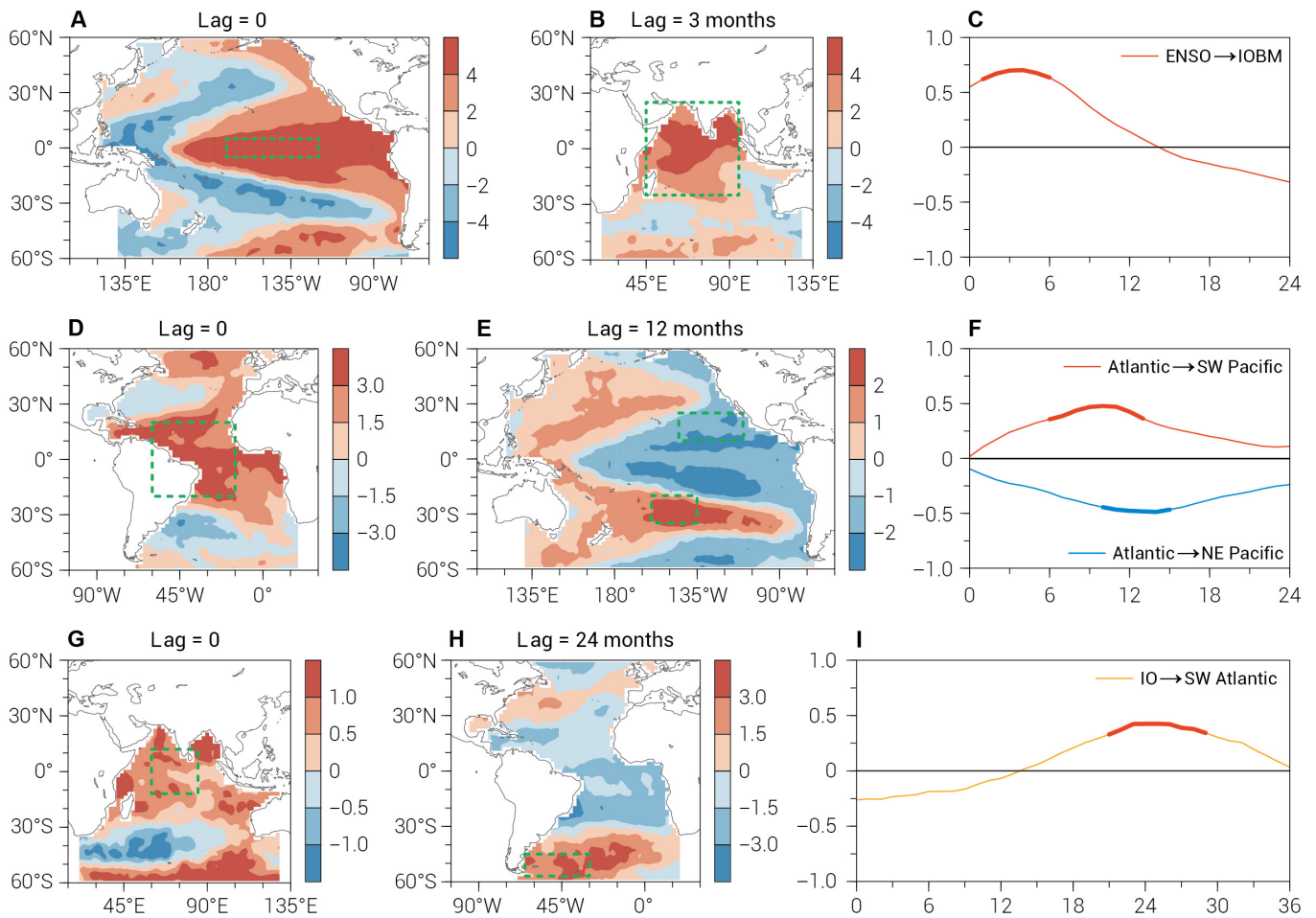


**Fig. 3.** Patterns of cross-basin interaction at different time delays. Singular value decomposition (SVD) analysis results for (A and B) preceding Pacific sea surface temperature (SST) anomalies and lagged Indian Ocean (IO) SST anomalies at a lag of 3 months, (D and E) preceding Atlantic SST anomalies and lagged Pacific SST anomalies at a lag of 12 months, and (G and H) preceding Indian Ocean SST anomalies and lagged Atlantic SST anomalies at a lag of 24 months. Left singular vectors are shown in (A), (D), and (G), while right singular vectors are shown in (B), (E), and (H). Lead-lag correlation coefficients between (C) equatorial central Pacific Ocean (5°S to 5°N, 170°W to 120°W) and Indian Ocean (25°S to 25°N, 45° to 95°E), (F) tropical Atlantic Ocean (20°S to 20°N, 60° to 15°W) and subtropical northeastern (NE) Pacific Ocean (10° to 25°N, 145° to 110°W) (red line), tropical Atlantic Ocean and subtropical southwestern (SW) Pacific Ocean (35° to 20°S, 160° to 135°W) (blue line), and (I) tropical Indian Ocean (12°S to 12°N, 60° to 85°E) and subpolar southwestern Atlantic Ocean (57° to 45°S, 65° to 30°W). Significant correlation coefficients ( $P < 0.05$ ) are denoted by thick lines in (C), (F), and (I).

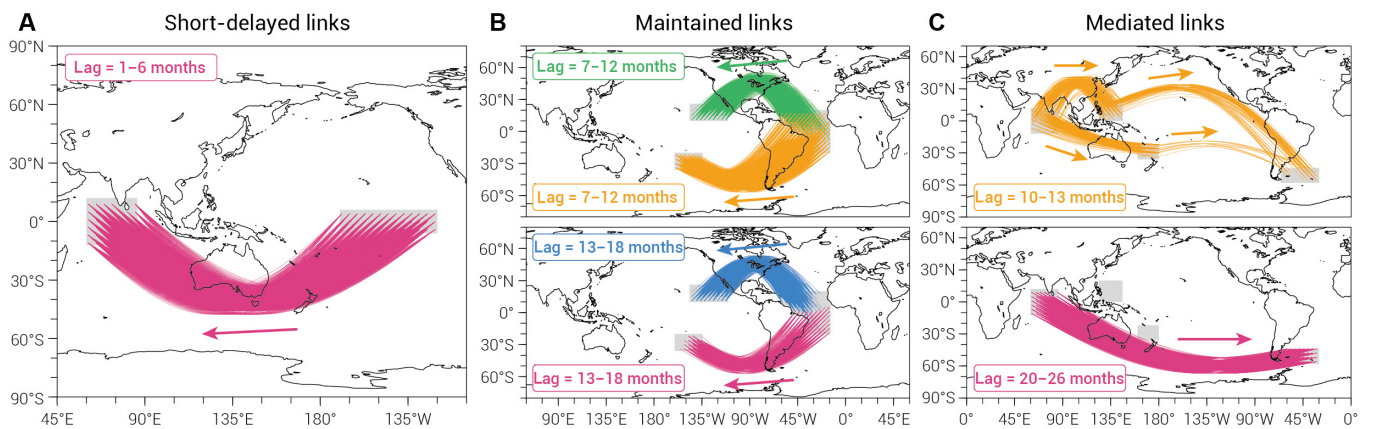


**Fig. 4.** Schematic diagrams of alternating interbasin sea surface temperature (SST) connections among the Pacific, Atlantic, and Indian oceans. (A) Pink lines indicate the significant links from the equatorial central Pacific Ocean (5°S to 5°N, 170°W to 120°W) to the tropical Indian Ocean (12°S to 12°N, 60° to 85°E) for the time lags of 1 to 6 months. (B) Colored lines indicate the significant links from the tropical Atlantic Ocean (20°S to 20°N, 60° to 15°W) to the subtropical northeastern Pacific Ocean (10° to 25°N, 145° to 110°W) and the subtropical southern Pacific Ocean (35° to 20°S, 160° to 135°W), respectively, for the time lags of 7 to 12 months (top) and 13 to 18 months (bottom). (C) Colored lines indicate the significant links from the tropical Indian Ocean to the subpolar southwestern Atlantic Ocean (57° to 45°S, 65° to 30°W) for the time lags of 20 to 26 months (bottom). Short-delayed links mediated by the tropical northwestern Pacific (0° to 20°N, 125° to 145°E) and subtropical southwestern Pacific (35° to 22°S, 160°E to 180°) for the time lags of 10 to 13 months are also shown in the top panel of (C). Colored curves are plotted only when at least 3 significant links (i.e., significant for at least 3 lags) occur between 2 grid cells during the respective lag periods.

Downloaded from https://spj.science.org at Wissenschaftspark Albert Einstein on April 07, 2026

South Pacific via the ITF or the Tasman leakage [32,83], and these anomalies may subsequently be transmitted to the sub-polar southwestern Atlantic through the Antarctic Circumpolar Current [84,85].

### Simulations and projections by 34 CMIP6 models

To explore how the alternating connectivity among the Indian, Pacific, and Atlantic oceans evolves under warming conditions, we calculated the network degree divergence using historical and SSP5-8.5 scenario simulations from 34 CMIP6 models. Model skill was first evaluated against observed interbasin teleconnection. The multimodel ensemble (MME) mean of historical simulations reproduced short-lag connections, particularly the dominant Pacific influence on the Indian Ocean within 6 months (Fig. 5A). However, the MME mean failed to capture interactions among the 3 basins at longer lags, especially those originating from the Atlantic (Fig. 5A versus Fig. 1A). This limitation is linked to the mean-state SST biases in the Atlantic Ocean. The MME exhibits a pronounced cold SST bias over the tropical western North Atlantic warm pool region compared with observations (see Fig. S1B), where SST anomalies play a key role in initiating the atmospheric convection anomalies that mediate Atlantic influences on the Pacific and Indian oceans. Such cold biases suppress local convection and weaken SST–precipitation coupling, thereby reducing the ability of the models to simulate longer-lag Atlantic-originated interbasin connections. To identify higher-performing models, we selected 4 models based on significant correlation with observations ( $r > 0.3$  for all 3 series): BCC-CSM2-MR, CAMS-CSM1-0, EC-Earth3, and KOIST-ESM (Fig. 5B). Compared with

the MME, these models show a reduction in cold bias in the tropical western North Atlantic, providing a more realistic mean-state SST background. As a result, they better simulated Atlantic-to-Pacific influences during the second lag period (7 to 19 months), although simulated signals remained weaker in magnitude than the observations (Fig. 5B versus Fig. 1A).

Under SSP5-8.5, interactions among the 3 oceans are projected to intensify by the late 21st century (Fig. 5C and D). Strengthening appears in both the full 34-model ensemble (Fig. 5C) and the subset of 4 higher-performing models (Fig. 5D). Intensification is reflected in increased numbers of significant links and higher average link strength (Fig. S2). A plausible mechanism involves changes in both the mean and variability of SST under global warming. It has been argued that the warming of the tropical mean SSTs will increase the sensitivity of deep convection to SST anomalies, enabling stronger convective rainfall [86,87]. Intensified precipitation drives more vigorous atmospheric circulation, reinforcing atmospheric teleconnection pathways. In addition, concurrent upper ocean warming strengthens stratification, amplifying thermocline responses to wind forcing [88,89]. This enhanced oceanic adjustment magnifies local air–sea interactions triggered by remote SST-induced atmospheric circulation anomalies. Intermodel correlations between changes in SST variance and interbasin link numbers also indicated that models with larger future increases in SST variability tend to exhibit stronger enhancements in interbasin connectivity (Fig. S3), suggesting that the amplified SST variability under global warming contributes substantially to strengthened 3-ocean linkages.

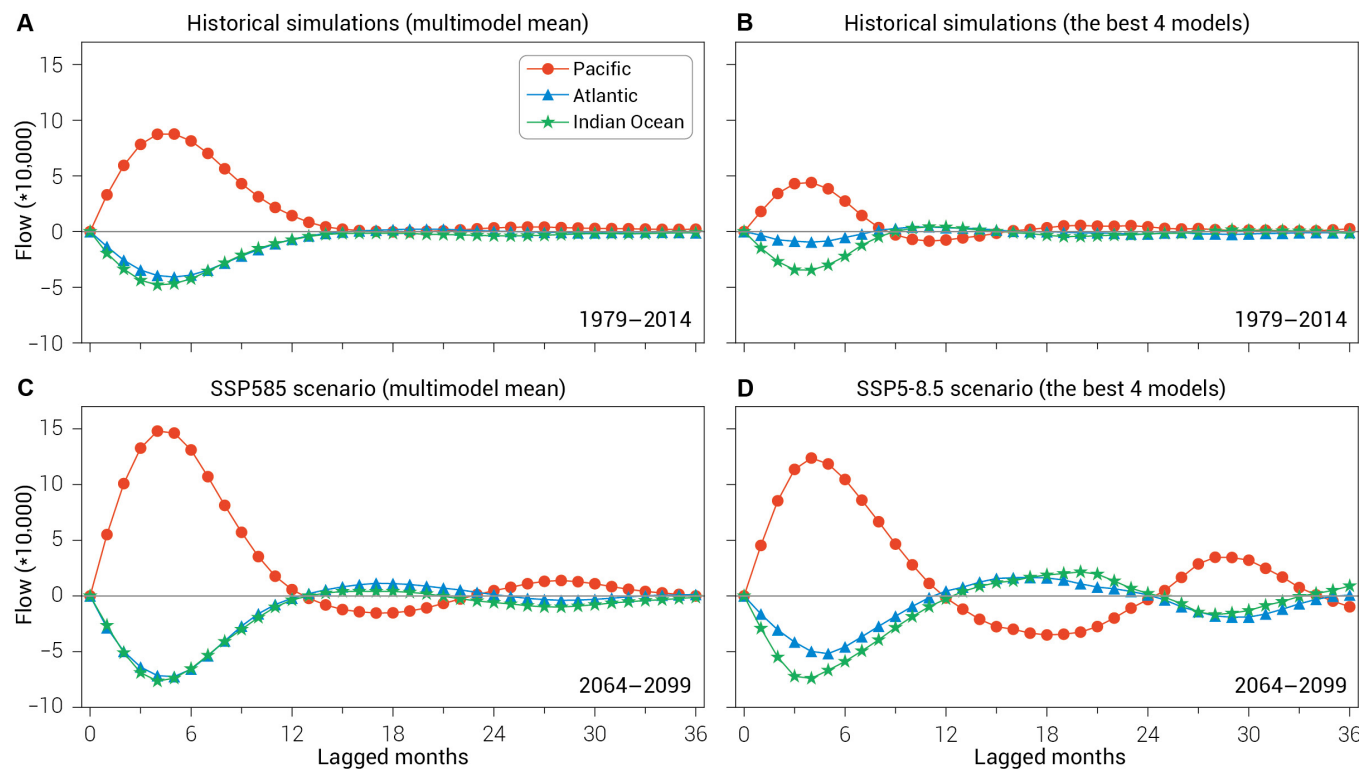


**Fig. 5.** Model simulations and projections of signal flows among the 3 oceans. Network degree divergence for the Pacific Ocean (red line with circles), Atlantic Ocean (blue line with triangles), and Indian Ocean (green line with pentagrams) in (A and B) the historical simulations for 1979–2014 and (C and D) the SSP5-8.5 scenario projections for 2064–2099. The multimodel mean of 34 Coupled Model Intercomparison Project Phase 6 (CMIP6) models is shown in (A) and (C), and the average of the 4 best models—BCC-CSM2-MR, CAMS-CSM1-0, EC-Earth3, and KOIST-ESM—is shown in (B) and (D). All 3 ocean lines of the best 4 models exhibit correlation coefficients greater than 0.3 with the 3 ocean lines of observations.

## Discussion

Using complex network analyses, this study reveals a sequential pattern of dominant interbasin SST influences among the Pacific, Atlantic, and Indian oceans. At time lags shorter than 6 months, Pacific Ocean impacts on the Indian Ocean are most pronounced. During lags of 7 to 19 months, Atlantic influences on the Pacific become dominant, while longer delays highlight signals from the Indian and Pacific oceans toward the Atlantic Ocean. The MME mean of 34 CMIP6 models can capture short-lag Pacific dominance but fail to reproduce medium- and long-lag connections. Nevertheless, the 4 CMIP6 models (BCC-CSM2-MR, CAMS-CSM1-0, EC-Earth3, and KOIST-ESM) reasonably simulate the observed alternating connectivity. Both the 4 selected models and the full ensemble project intensified alternating connections among the 3 oceans by the end of the 21st century under SSP5-8.5.

While our data-driven framework (i.e., complex network) reveals an alternating interbasin connectivity and its intensification in the warmer future, the specific mechanisms for these remote SST connections are not thoroughly explored in this study. Each ocean basin hosts multiple distinct modes of SST variability, whose interplay likely contributes to the complexity of cross-basin linkages, underscoring the need for further dynamical investigations.

Previous studies have shown that ENSO displays strong quasi-biennial characteristics, while the Atlantic and Indian oceans can act as capacitors excited by ENSO, subsequently providing feedback into ENSO evolution. Lead-lag SST relationships inferred from statistical analyses may therefore reflect spurious linkage arising from ENSO autocorrelation [90–92]. However, the present network results reveal a systematic, lag-dependent shift in the dominant source regions, together with basin-scale and off-equatorial spatial structures that differ substantially from the canonical ENSO SST patterns (Fig. 3E). These features are inconsistent with a simple ENSO recharge or quasi-biennial echo projecting back onto the Pacific at a fixed phase lag and instead point to more complex pan-oceanic interactions operating across multiple time scales.

Nevertheless, it must be acknowledged that the statistically significant connections identified by the network analysis represent temporal precedence and coordinated variability, rather than definitive physical causality. Therefore, the inferred interbasin links should be interpreted as lag-dependent basin-scale interaction patterns that highlight where and when coordinated SST evolution occurs, guiding targeted dynamic diagnostics and sensitivity experiments. Despite this limitation, our results highlight the utility of complex network approaches in diagnosing global ocean connectivity. The strengthened interbasin linkages under global warming may offer a pathway toward enhanced predictability of the global oceans because SST signals in one ocean can lead those in other oceans. Such strengthened links could potentially extend the predictability of terrestrial climate, enabling forecasts based on SST anomalies, including those related to El Niño. To gain a deeper understanding, further analysis using complex networks should consider the couplings between the oceans and the atmosphere, which play a crucial role in regulating the global climate.

## Acknowledgments

We thank J. Kurths and D. Gerten of the Potsdam Institute for Climate Impact Research for helpful conversations. F.C.

gratefully acknowledges the China Scholarship Council scholarship.

**Funding:** This study was supported by the Guangdong Major Project of Basic and Applied Basic Research (grant 2020B0301030004), the National Natural Science Foundation of China (grants 42505021 and 42088101), the Southern Marine Science and Engineering Guangdong Laboratory (Zhuhai) (SML2023SP209), the Guangdong Province Key Laboratory for Climate Change and Natural Disaster Studies (2023B1212060019), and the Postdoctoral Fellowship Program of China Postdoctoral Science Foundation (GZC20250218).

**Author contributions:** F.C.: Conceptualization, methodology, formal analysis, visualization, and original draft preparation. S.Y.: Conceptualization, writing review and editing, and funding acquisition. S.L.: Conceptualization, methodology, formal analysis, visualization, and original draft preparation. T.Z.: Conceptualization, methodology, review, and editing.

**Competing interests:** The authors declare that they have no competing interests.

## Data Availability

The HadISST1 data are available at <https://www.metoffice.gov.uk/hadobs/hadisst/data/download.html>. The outputs of the CMIP6 simulations were obtained from <https://esgf-node.llnl.gov/search/cmip6/>.

## Supplementary Materials

Table S1  
Figs. S1 to S3

## References

1. Trenberth KE, Branstator GW, Karoly D, Kumar A, Lau NC, Ropelewski C. Progress during TOGA in understanding and modeling global teleconnections associated with tropical sea surface temperatures. *J Geophys Res Ocean*. 1998;103(C7):14291–14324.
2. Shukla J, Anderson J, Baumhefner D, Brankovic C, Chang Y, Kalnay E, Marx L, Palmer T, Paolino D, Ploshay J, et al. Dynamical seasonal prediction. *Bull Am Meteorol Soc*. 2000;81(11):2593–2606.
3. Von Schuckmann K, Cheng L, Palmer MD, Hansen J, Tassone C, Aich V, Adusumilli S, Beltrami H, Boyer T, José Cuesta-Valero F, et al. Heat stored in the Earth system: Where does the energy go? *Earth Syst Sci Data*. 2020;12(4):2013–2041.
4. Cai W, Wu L, Lengaigne M, Li T, McGregor S, Kug JS, Yu JY, Stuecker MF, Santoso A, Li X, et al. Pantropical climate interactions. *Science*. 2019;363(6430):Article eaav4236.
5. Wang C. Three-ocean interactions and climate variability: A review and perspective. *Clim Dyn*. 2019;53(7):5119–5136.
6. Richter I, Chang P, Chiu PG, Danabasoglu G, Doi T, Dommenges D, Gastineau G, Gillett ZE, Hu A, Kataoka T, et al. The Tropical Basin Interaction Model Intercomparison Project (TBIMIP). *Geosci Model Dev*. 2025;18(9):2587–2608.
7. Webster PJ, Yang S. Monsoon and ENSO: Selectively interactive systems. *Q J R Meteorol Soc*. 1992;118(507):877–926.
8. Yang S, Li Z, Yu JY, Hu X, Dong W, He S. El Niño-Southern Oscillation and its impact in the changing climate. *Natl Sci Rev*. 2018;5(6):840–857.

9. Lin S, Yang S, Dong B, Deng K, Fang K. Deciphering the intermodel spread in projections of the impacts of Indian summer monsoon on ENSO under global warming. *J Geophys Res Atmos*. 2025;130(4):e2024JD042803.
10. Lin S, Fang K, Wu H, Fan H, Zhou F, Li J, Deng K, Linderholm HW, Yang S. Multidecadal modulation of multi-year El Niño events over the past millennium. *Sci China Earth Sci*. 2025;68(9):2827–2838.
11. Annamalai H, Kida S, Hafner J. Potential impact of the tropical Indian Ocean-Indonesian seas on El Niño characteristics. *J Clim*. 2010;23(14):3933–3952.
12. Izumo T, Vialard J, Lengaigne M, De Boyer Montegut C, Behera SK, Luo JJ, Cravatte S, Masson S, Yamagata T. Influence of the state of the Indian Ocean dipole on the following years El Niño. *Nat Geosci*. 2010;3(3):168–172.
13. Ham YG, Kug JS, Park JY, Jin FF. Sea surface temperature in the north tropical Atlantic as a trigger for El Niño/Southern Oscillation events. *Nat Geosci*. 2013;6(2):112–116.
14. Wang J-Z, Wang C. Joint boost to super El Niño from the Indian and Atlantic oceans. *J Clim*. 2021;34(12):4937–4964.
15. Fan H, Wang C, Yang S, Zhang G. Coupling is key for the tropical Indian and Atlantic oceans to boost super El Niño. *Sci Adv*. 2024;10(37):Article eadp2281.
16. Sun M, Chen L, Li T, Luo JJ. CNN-based ENSO forecasts with a focus on SSTA zonal pattern and physical interpretation. *Geophys Res Lett*. 2023;50(20):e2023GL105175.
17. Alexander MA, Bladé I, Newman M, Lanzante JR, Lau NC, Scott JD. The atmospheric bridge: The influence of ENSO teleconnections on air-sea interaction over the global oceans. *J Clim*. 2002;15(16):2205–2231.
18. Lin S, Yang S, He S, Li Z, Chen J, Dong W, Wu J. Attribution of the seasonality of atmospheric heating changes over the western tropical Pacific with a focus on the spring season. *Clim Dyn*. 2022;58(9):2575–2592.
19. Li M, Gordon AL, Gruenburg LK, Wei J, Yang S. Interannual to decadal response of the Indonesian Throughflow vertical profile to Indo-Pacific forcing. *Geophys Res Lett*. 2020;47(11):Article e2020GL087679.
20. Saji NH, Goswami BN, Vinayachandran PN, Yamagata T. A dipole mode in the tropical Indian ocean. *Nature*. 1999;401(6751):360–363.
21. Webster PJ, Moore AM, Loschnigg JP, Leben RR. Coupled ocean-atmosphere dynamics in the Indian Ocean during 1997–98. *Nature*. 1999;401(6751):356–360.
22. Behera SK, Luo JJ, Masson S, Rao SA, Sakuma H, Yamagata T. A CGCM study on the interaction between IOD and ENSO. *J Clim*. 2006;19(9):1688–1705.
23. Klein SA, Soden BJ, Lau NC. Remote sea surface temperature variations during ENSO: Evidence for a tropical atmospheric bridge. *J Clim*. 1999;12(4):917–932.
24. Yang J, Liu Q, Xie SP, Liu Z, Wu L. Impact of the Indian Ocean SST basin mode on the Asian summer monsoon. *Geophys Res Lett*. 2007;34(2):Article 2006GL028571.
25. Xie SP, Hu K, Hafner J, Tokinaga H, Du Y, Huang G, Sampe T. Indian Ocean capacitor effect on Indo-Western Pacific climate during the summer following El Niño. *J Clim*. 2009;22(3):730–747.
26. Feng M, McPhaden MJ, Xie SP, Hafner J. La Niña forces unprecedented Leeuwin current warming in 2011. *Sci Rep*. 2013;3(1):Article 1277.
27. Ohba M, Ueda H. An impact of SST anomalies in the Indian Ocean in acceleration of the El Niño to La Niña transition. *J Meteorol Soc Japan*. 2007;85(3):335–348.
28. Izumo T, Vialard J, Dayan H, Lengaigne M, Suresh I. A simple estimation of equatorial Pacific response from windstress to untangle Indian Ocean dipole and basin influences on El Niño. *Clim Dyn*. 2016;46(7):2247–2268.
29. Wu J, Fan H, Lin S, Zhong W, He S, Keenlyside N, Yang S. Boosting effect of strong western pole of the Indian Ocean dipole on the decay of El Niño events. *npj Clim Atmos Sci*. 2024;7:6.
30. Zhong Y, Lin W, Zhang T, Yuan D, Yang S, Lin S, Yu W. Role of the spring sea surface temperature over the southeastern Indian Ocean in bridging the Indian Ocean dipole and subsequent ENSO. *J Clim*. 2025;38(5):1305–1317.
31. Zhong Y, Lin W, Yuan D, Zhang T, Yang S, Lin S, Yu W. Precursorship between the Indian Ocean dipole and the following year ENSO in the CMIP6 simulations. *Clim Dyn*. 2026;64(1):Article 8.
32. Yuan D, Wang J, Xu T, Xu P, Hui Z, Zhao AX, Luan Y, Zheng W, Yu Y. Forcing of the Indian Ocean dipole on the interannual variations of the tropical Pacific Ocean: Roles of the Indonesian Throughflow. *J Clim*. 2011;24(14):3593–3608.
33. Yuan D, Zhou H, Zhao X. Interannual climate variability over the tropical Pacific ocean induced by the Indian Ocean dipole through the Indonesian Throughflow. *J Clim*. 2013;26(9):2845–2861.
34. Saji NH, Yamagata T. Possible impacts of Indian Ocean dipole mode events on global climate. *Clim Res*. 2003;25(2):151–169.
35. Cai W, van Rensch P, Cowan T, Hendon HH. Teleconnection pathways of ENSO and the IOD and the mechanisms for impacts on Australian rainfall. *J Clim*. 2011;24(15):3910–3923.
36. Chiang JCH, Sobel AH. Tropical tropospheric temperature variations caused by ENSO and their influence on the remote tropical climate. *J Clim*. 2002;15(18):2616–2631.
37. Wang C, Kucharski F, Barimalala R, Bracco A. Teleconnections of the tropical Atlantic to the tropical Indian and Pacific oceans: A review of recent findings. *Meteorol Zeitschrift*. 2009;18(4):445–454.
38. Wallace JM, Gutzler DS. Teleconnections in the geopotential height field during the Northern Hemisphere winter. *Mon Weather Rev*. 1981;109(4):784–812.
39. Alexander M, Scott J. The influence of ENSO on air-sea interaction in the Atlantic. *Geophys Res Lett*. 2002;29(14):46–41.
40. García-Serrano J, Cassou C, Douville H, Giannini A, Doblas-Reyes FJ. Revisiting the ENSO teleconnection to the tropical North Atlantic. *J Clim*. 2017;30(17):6945–6957.
41. Jiang L, Li T. Relative roles of El Niño-induced extratropical and tropical forcing in generating tropical North Atlantic (TNA) SST anomaly. *Clim Dyn*. 2019;53(7):3791–3804.
42. Wang L, Yu JY, Paek H. Enhanced biennial variability in the Pacific due to Atlantic capacitor effect. *Nat Commun*. 2017;8(1):Article 14887.
43. Jiang L, Li T, Ham Y. Critical role of tropical North Atlantic SSTA in boreal summer in affecting subsequent ENSO evolution. *Geophys Res Lett*. 2022;49(8):Article e2021GL097606.
44. Polo I, Martin-Rey M, Rodriguez-Fonseca B, Kucharski F, Mechoso CR. Processes in the Pacific La Niña onset triggered by the Atlantic Niño. *Clim Dyn*. 2015;44(1):115–131.
45. Zhang G, Chen J, Fan H, Zhang L, Chen M, Wang X, Wang D. Unveiling the role of south tropical Atlantic in winter Atlantic Niño inducing La Niña. *Nat Commun*. 2025;16(1):1612.
46. Wang R, He J, Luo JJ, Chen L. Atlantic warming enhances the influence of Atlantic Niño on ENSO. *Geophys Res Lett*. 2024;51(8):Article e2023GL108013.

47. Wang R, Chen L, Luo J-J, Sun M. Unveiling the impacts of winter Atlantic Niño/Niña on the ENSO decay pace. *Environ Res Lett.* 2025;20(10):Article 104016.
48. Wang R, Chen L, Li T, Luo J-J. Atlantic Niño/Niña prediction skills in NMME models. *Atmosphere.* 2021;12(7):803.
49. Yu J, Li T, Tan Z, Zhu Z. Effects of tropical North Atlantic SST on tropical cyclone genesis in the western North Pacific. *Clim Dyn.* 2016;46:865–877.
50. Li X, Xie S-P, Gille ST, Yoo C. Atlantic-induced pan-tropical climate change over the past three decades. *Nat Clim Change.* 2016;6:275–279.
51. Jiang L, Li T. Impacts of tropical North Atlantic and equatorial Atlantic SST anomalies on ENSO. *J Clim.* 2021;34(14):5635–5655.
52. Zhang L, Han W. Indian Ocean dipole leads to Atlantic Niño. *Nat Commun.* 2021;12(1):5952.
53. Chen S, Chen W, Xie S-P, Yu B, Wu R, Wang Z, Lan X, Graf H-F. Strengthened impact of boreal winter North Pacific oscillation on ENSO development in warming climate. *npj Clim Atmos Sci.* 2024;7:69.
54. Fan H, Yang S, Wang C, Lin S. Revisiting the impacts of tropical Pacific SST anomalies on the Pacific Meridional Mode during the decay of strong eastern Pacific El Niño events. *J Clim.* 2023;36(15):4987–5002.
55. Yu W, Wang D, Liu Y, Chen D, Lin S, Peng Y. Impacts of North Atlantic tripole SSTAs mode and its three individual components on ENSO check for updates. *npj Clim Atmos Sci.* 2025;8:373.
56. Runge J, Petoukhov V, Kurths J. Quantifying the strength and delay of climatic interactions: The ambiguities of cross correlation and a novel measure based on graphical models. *J Clim.* 2014;27(2):720–739.
57. Kretschmer M, Coumou D, Donges JF, Runge J. Using causal effect networks to analyze different arctic drivers of midlatitude winter circulation. *J Clim.* 2016;29(11):4069–4081.
58. McGraw MC, Barnes EA. Memory matters: A case for granger causality in climate variability studies. *J Clim.* 2018;31(8):3289–3300.
59. McGregor S, Stuecker MF, Kajtar JB, England MH, Collins M. Model tropical Atlantic biases underpin diminished Pacific decadal variability. *Nat Clim Change.* 2018;8(6):493–498.
60. Luo J-J, Wang G, Dommenget D. May common model biases reduce CMIP5's ability to simulate the recent Pacific La Niña-like cooling? *Clim Dyn.* 2018;50(3-4):1335–1351.
61. Lin S, Dong B, Yang S, He S, Hu Y. Causes of diverse impacts of ENSO on the southeast Asian summer monsoon among CMIP6 models. *J Clim.* 2024;37(2):419–438.
62. Fang Y, Screen JA, Hu X, Lin S, Williams NC, Song Y. CMIP6 models underestimate ENSO teleconnections in the southern hemisphere. *Geophys Res Lett.* 2024;51(18):| Article e2024GL110738.
63. Boers N, Goswami B, Rheinwalt A, Bookhagen B, Hoskins B, Kurths J. Complex networks reveal global pattern of extreme-rainfall teleconnections. *Nature.* 2019;566(7744):373–377.
64. Li K, Huang Y, Liu K, Wang M, Cai F, Zhang J, Boers N. Key propagation pathways of extreme precipitation events revealed by climate networks. *npj Clim Atmos Sci.* 2024;7:165.
65. Cai F, Liu C, Gerten D, Yang S, Zhang T, Li K, Kurths J. Sketching the spatial disparities in heatwave trends by changing atmospheric teleconnections in the Northern Hemisphere. *Nat Commun.* 2024;15:8012.
66. Liu C, Galfi VM, Cai F, Robinson WA, Coumou D. The role of Rossby wave dynamics in spatially compounding heatwaves in mid-summer 2023. *Environ Res Lett.* 2025;20(3):034052.
67. Cai F, Lin S, Gerten D, Yang S, Jiang X, Su Z, Kurths J. Intensified dominance of El Niño-like convection relevant for global atmospheric circulation variations. *npj Clim Atmos Sci.* 2025;8:242.
68. Meng J, Fan J, Ludescher J, Agarwal A, Chen X, Bunde A, Kurths J, Schellnhuber HJ. Complexity-based approach for El Niño magnitude forecasting before the spring predictability barrier. *Proc Natl Acad Sci USA.* 2020;117(1):177–183.
69. Lu Z, Yuan N, Yang Q, Ma Z, Kurths J. Early warning of the Pacific decadal oscillation phase transition using complex network analysis. *Geophys Res Lett.* 2021;48(7):Article e2020GL091674.
70. Lu Z, Dong W, Lu B, Yuan N, Ma Z, Bogachev MI, Kurths J. Early warning of the Indian Ocean dipole using climate network analysis. *Proc Natl Acad Sci USA.* 2022;119(11): Article e2109089119.
71. Rayner NA, Parker DE, Horton EB, Folland CK, Alexander LV, Rowell DP, Kent EC, Kaplan A. Global analyses of sea surface temperature, sea ice, and night marine air temperature since the late nineteenth century. *J Geophys Res Atmos.* 2003;108(D14):4407.
72. Eyring V, Bony S, Meehl GA, Senior CA, Stevens B, Stouffer RJ, Taylor KE. Overview of the Coupled Model intercomparison Project Phase 6 (CMIP6) experimental design and organization. *Geosci Model Dev.* 2016;9(5):1937–1958.
73. Hu ZZ, Kumar A, Xue Y, Jha B. Why were some La Niñas followed by another La Niña? *Clim Dyn.* 2014;42:1029–1042.
74. DiNezio PN, Deser C. Nonlinear controls on the persistence of La Niña. *J Clim.* 2014;27(19):7335–7355.
75. Ding H, Keenlyside NS, Latif M. Impact of the equatorial Atlantic on the El Niño southern oscillation. *Clim Dyn.* 2012;38:1965–1972.
76. Chikamoto Y, Johnson ZF, Wang S-YS, McPhaden MJ, Mochizuki T. El Niño–Southern Oscillation evolution modulated by Atlantic forcing. *J Geophys Res Ocean.* 2020;125(8):e2020JC016318.
77. Meehl GA. The south Asian monsoon and the tropospheric biennial oscillation. *J Clim.* 1997;10(8):1921–1943.
78. Meehl GA, Arblaster JM, Loschnigg J. Coupled ocean-atmosphere dynamical processes in the tropical Indian and Pacific oceans and the TBO. *J Clim.* 2003;16(13):2138–2158.
79. Li T, Liu P, Fu X, Wang B, Meehl GA. Spatiotemporal structures and mechanisms of the tropospheric biennial oscillation in the Indo-Pacific warm ocean regions. *J Clim.* 2006;19(13):3070–3087.
80. Wang B, Wu R, Lukas R, An S-I. A possible mechanism for ENSO turnabouts. *Dyn Atmos Gen Circ Clim.* 2001;552–578.
81. Li Z, Yang S, Hu X, Dong W, He B. Change in long-lasting El Niño events by convection-induced wind anomalies over the western Pacific in boreal spring. *J Clim.* 2018;31(10): 3755–3763.
82. Lin S, Yang S, He S, Fan H, Chen J, Dong W, Wu J, Guan Y. Atmospheric–oceanic processes over the Pacific involved in the effects of the Indian summer monsoon on ENSO. *J Clim.* 2023;36(17):6021–6043.
83. van Sebille E, Sprintall J, Schwarzkopf FU, Sen Gupta A, Santoso A, England MH, Biastoch A, Böning CW. Pacific-to-Indian Ocean connectivity: Tasman leakage, Indonesian Throughflow, and the role of ENSO. *J Geophys Res Ocean.* 2014;119(2):1365–1382.
84. Garzoli SL, Matano R. The South Atlantic and the Atlantic meridional overturning circulation. *Deep Res Part II Top Stud Oceanogr.* 2011;58(17-18):1837–1847.

85. Rousselet L, Cessi P, Forget G. Routes of the upper branch of the Atlantic meridional overturning circulation according to an ocean state estimate. *Geophys Res Lett.* 2020;47(18): Article e2020GL089137.
86. Power S, Delage F, Chung C, Kociuba G, Keay K. Robust twenty-first-century projections of El Niño and related precipitation variability. *Nature.* 2013;502(7472): 541–545.
87. Lin S, Dong B, Yang S. Enhanced impacts of ENSO on the southeast Asian summer monsoon under global warming and associated mechanisms. *Geophys Res Lett.* 2024;51(2): Article e2023GL106437.
88. DiNezio PN, Clement AC, Vecchi GA, Soden BJ, Kirtman BP, Lee S-K. Climate response of the equatorial Pacific to global warming. *J Clim.* 2009;22(18):4873–4892.
89. Cai W, Wang G, Dewitte B, Wu L, Santoso A, Takahashi K, Yang Y, Carréric A, McPhaden MJ. Increased variability of eastern Pacific El Niño under greenhouse warming. *Nature.* 2018;564(7735):201–206.
90. Stuecker MF, Timmermann A, Jin FF, Chikamoto Y, Zhang W, Wittenberg AT, Widiasih E, Zhao S. Revisiting ENSO/ Indian Ocean dipole phase relationships. *Geophys Res Lett.* 2017;44(5):2481–2492.
91. Zhang W, Jiang F, Stuecker MF, Jin FF, Timmermann A. Spurious north tropical Atlantic precursors to El Niño. *Nat Commun.* 2021;12(1):3096.
92. Jiang F, Zhang W, Jin FF, Stuecker MF, Timmermann A, McPhaden MJ, Boucharel J, Wittenberg AT. Resolving the tropical Pacific/Atlantic interaction conundrum. *Geophys Res Lett.* 2023;50(13):e2023GL103777.

# Ocean - Land - Atmosphere Research

A SCIENCE PARTNER JOURNAL

## Alternating Connectivity with Temporal Delays between the Pacific, Atlantic, and Indian Oceans

Fenyng Cai, Song Yang, Shuheng Lin, and Tuantuan Zhang

**Citation:** Cai F, Yang S, Lin S, Zhang T. Alternating Connectivity with Temporal Delays between the Pacific, Atlantic, and Indian Oceans. *Ocean-Land-Atmos Res.* 2026;5:0142. DOI: 10.34133/olar.0142

Sea surface temperature (SST) variability interacts dynamically across the Pacific, Atlantic, and Indian oceans, exerting pronounced influence on global climate. However, the mechanism of signal transmission among these basins remains unclear. Using complex network analysis of lead-lag SST connections, results indicate that dominant interannual influences shift sequentially across the Pacific, Atlantic, and Indian oceans. At short-term lags (#6 months), the Pacific strongly affects the Indian Ocean. For medium-term lags (7 to 19 months), the Atlantic exerts greater influence on the Pacific. At long-term lags (#20 months), pronounced SST connections emerge from both the Indian and Pacific oceans toward the Atlantic. Coupled Model Intercomparison Project Phase 6 models capture short-term Pacific impacts effectively, but only a limited subset reproduces medium- and long-term interbasin linkages. Furthermore, model projections consistently suggest intensification of these cross-basin interactions under future warming scenarios. Quantitative evaluation of lead-lag signal flow among oceans enhances understanding of interbasin interactions and large-scale climate variability.

Image

**View the article online**

<https://spj.science.org/doi/10.34133/olar.0142>

Use of this article is subject to the [Terms of service](#)

---

*Ocean-Land-Atmosphere Research* (ISSN 2771-0378) is published by the American Association for the Advancement of Science. 1200 New York Avenue NW, Washington, DC 20005.

Copyright © 2026 Fenyng Cai et al.

Exclusive licensee Southern Marine Science and Engineering Guangdong Laboratory (Zhuhai). No claim to original U.S. Government Works. Distributed under a [Creative Commons Attribution License \(CC BY 4.0\)](#).